




## Open Archive Toulouse Archive Ouverte (OATAO)

OATAO is an open access repository that collects the work of Toulouse researchers and makes it freely available over the web where possible

This is an author's version published in: <http://oatao.univ-toulouse.fr/26124>

**Official URL:** <https://doi.org/10.1080/1536383X.2020.1749051>

### To cite this version:

Lobiak, Egor V. and Kuznetsova, Viktoriia R. and Flahaut, Emmanuel  and Okotrub, Alexander V. and Bulusheva, Lyubov G. *Effect of Co-Mo catalyst preparation and CH<sub>4</sub>/H<sub>2</sub> flow on carbon nanotube synthesis*. (2020) *Fullerenes Nanotubes and Carbon Nanostructures*, 28 (9). 1-9. ISSN 1536-383X

Any correspondence concerning this service should be sent to the repository administrator: [tech-oatao@listes-diff.inp-toulouse.fr](mailto:tech-oatao@listes-diff.inp-toulouse.fr)

# Effect of Co-Mo catalyst preparation and CH<sub>4</sub>/H<sub>2</sub> flow on carbon nanotube synthesis

Egor V. Lobiak<sup>a</sup>, Viktoriia R. Kuznetsova<sup>a,b</sup>, Emmanuel Flahaut<sup>c</sup>, Alexander V. Okotrub<sup>a</sup>, and Lyubov G. Bulusheva<sup>a</sup>

<sup>a</sup>Nikolaev Institute of Inorganic Chemistry SB RAS, Novosibirsk, Russia; <sup>b</sup>Novosibirsk State Technical University, Novosibirsk, Russia; <sup>c</sup>CIRIMAT, Université de Toulouse, CNRS, INPT, UPS, UMR CNRS-UPS-INP N°5085, Université Toulouse 3 Paul Sabatier, Bât. CIRIMAT, Toulouse cedex 9, France

## ABSTRACT

Supported Co-Mo catalysts with a given ratio of metals were prepared from polyoxomolybdate Mo<sub>12</sub>O<sub>28</sub>(μ<sub>2</sub>-OH)<sub>12</sub>{Co(H<sub>2</sub>O)<sub>3</sub>}<sub>4</sub> using impregnation and combustion methods. Effects of the type of catalyst and the ratio and flow of methane and hydrogen gases on the structure of carbon nanotubes (CNTs) synthesized by catalytic chemical vapor deposition (CCVD) method were studied using transmission electron microscopy and Raman spectroscopy. The catalyst prepared by combustion method yielded mainly individualized CNTs, while the CNTs were highly entangled or bundled when impregnation method was used. In both cases, addition of hydrogen to methane led to reduction of the CNT yield. The samples synthesized using two different catalysts and the same CH<sub>4</sub>/H<sub>2</sub> ratio and flow of gases were tested in electrochemical capacitors. A higher specific surface area of the CNTs grown over impregnation-prepared catalyst caused a better performance at scan rates from 2 to 1000 mV/s.

## KEYWORDS

Carbon nanotubes; catalytic chemical vapor deposition; Co Mo catalyst; CH<sub>4</sub>/H<sub>2</sub> mixture; electrochemical capacitors

## 1. Introduction

Chemical vapor deposition (CVD) is a multivariable process, where any synthesis parameter may influence the target carbon product. The key parameter in the catalytic CVD (CCVD) synthesis of carbon nanotubes (CNTs) is the composition of the catalyst.<sup>[1]</sup> Transition metals such as Fe, Co, Ni and their alloys or with addition of Mo are common catalysts for this process. The efficiency of the catalyst for the growth of CNTs of different morphologies depends on the choice of the catalytic support, which allows controlling the size and distribution of catalytic metals.<sup>[2]</sup> The most often used supports are graphite, quartz, magnesium oxide, zeolite, alumina, silicon, silica<sup>[3]</sup> and less common substrates such as stainless steel, microfibrinous composite materials,<sup>[4]</sup> and glass mat<sup>[5]</sup> have also been reported. The interaction of the support with the active metal through van-der-Waals and electrostatic forces and/or surface groups affects the mobility and sintering of the metal<sup>[6]</sup> and thus modifies its activity.<sup>[1]</sup> For example, Chai et al.<sup>[7]</sup> showed that the performance of CoO catalyst for the growth of CNTs from methane at 700°C decreased as follows for oxide supports: Al<sub>2</sub>O<sub>3</sub> > CeO<sub>2</sub> > zeolite > SiO<sub>2</sub> > TiO<sub>2</sub> > CaO > MgO. The use of the MgO support for a Fe/Mo catalyst provided the highest yield of single-walled CNTs (SWCNTs) from methane at 850°C as compared to other supporting materials.<sup>[8]</sup>

There are several methods for the preparation of supported catalysts and among them are sol-gel, precipitation, impregnation and combustion. The impregnation is a simple method not requiring any specific equipment, where a porous support (MgO, CaO) is impregnated with a solution (usually aqueous) of metal salts, such as acetates,<sup>[9]</sup> nitrates<sup>[10]</sup> and ammonium heptamolybdate.<sup>[11]</sup> For example, the catalyst used in the well-known CoMoCat process for the synthesis of SWCNTs is prepared by impregnation of SiO<sub>2</sub> by an aqueous solution of Co(NO<sub>3</sub>)<sub>2</sub> and (NH<sub>4</sub>)<sub>6</sub>Mo<sub>7</sub>O<sub>24</sub> followed by drying in an oven at 80 °C and calcination at 500 °C.<sup>[12]</sup> Another common method is the combustion (fast thermal decomposition involving redox reactions) of a solution of metal salts with an organic reducing compound. Combustion of solutions of metal nitrates, ammonium heptamolybdate with citric acid or urea was used to produce the catalysts used for the synthesis of double-walled CNTs (DWCNTs).<sup>[13]</sup>

The first stage of the preparation of bi- or three-metallic catalyst is usually dissolution of metal-containing compounds used in the required ratio in a solvent.<sup>[1]</sup> An alternative way is to use compounds already containing two or more of the necessary metals. An example of such compounds is the giant polyoxomolybdate molecule with active transition metal and molybdenum atoms in a cluster core.<sup>[14]</sup> The first compound from this family used for the synthesis of CNTs was Keplerate, containing Fe and Mo

$[H_xPMo_{12}O_{40}CH_4Mo_{72}Fe_{30}(CH_3COO)_{15}O_{254}(H_2O)_{98}]$ .<sup>[15]</sup> The size of this molecule is 3 nm<sup>[16]</sup> and each molecule should on the principle produce a single metal nanoparticle for the growth of a CNT of a given structure. However, SWCNTs synthesized from methane at 900 °C exhibited a distribution of diameters.<sup>[15]</sup> The goal of selectivity was achieved by using  $Na_{15}[Na_3C\{Co(H_2O)_4\}_6\{WO(H_2O)\}_3(P_2W_{12}O_{48})_3]$ , which gave  $W_6Co_7$  catalysts for the synthesis of (14,4) chiral SWCNTs with a selectivity of 97%.<sup>[17]</sup> Thus, metal-containing cluster molecules can be a source of catalysts with well-controlled structures for the CCVD growth of high purity CNTs possessing a specific morphology and structure.

In the first work and subsequent investigations of polyoxomolybdate molecules for the preparation catalysts,  $SiO_2/Si$  substrates were used for deposition of molecules that resulted in very low yields of CNTs and created difficulties for their recovery by detachment from the substrate.<sup>[15,18,19]</sup> Edgar *et al.* for the first time distributed various Fe-containing polyoxomolybdates on  $MgO$  and  $Al_2O_3$  supports and obtained mixtures of SWCNTs and multi-walled CNTs (MWCNTs) from methane at a temperature of 1000 °C.<sup>[20]</sup> Similar results were achieved using the Keplerate with the  $Al_2O_3$  support<sup>[21]</sup> and  $MgO$  support.<sup>[22]</sup> Well-graphitized MWCNTs were obtained from  $C_2H_4/H_2$  at 900 °C using e-Keggin-type polyoxomolybdate clusters  $Mo_{12}O_{28}(\mu_2-OH)_{12}\{Ni(H_2O)_3\}_4$  and  $Mo_{12}O_{28}(\mu_2-OH)_{12}\{Co(H_2O)_3\}_4$  on  $MgO$  supports.<sup>[23]</sup> The use of supported polyoxomolybdates for the synthesis of CNTs is however still far from having been fully exploited.

One more important parameter in the CCVD synthesis is the gaseous carbon source, which is typically methane, ethylene, acetylene or carbon monoxide.<sup>[6]</sup> Conversion of a reaction gas to CNTs is always associated with the formation of various carbon by-products. Among the hydrocarbons, methane is the most thermodynamically stable and its pyrolysis yields only carbon and hydrogen atoms.<sup>[24]</sup> Thus, methane is often mixed with hydrogen to control the formation of unwanted carbon species in gas phase. In this point of view, it is important to determine the role of  $H_2$  in the CNT synthesis. One of the first studies on this topic was dealing with the arc-discharge synthesis process, where CNTs free of amorphous carbon were produced, but the role of  $H_2$  was not thoroughly discussed.<sup>[25]</sup> Later, decomposition of  $CH_4$  in an electric arc to  $C_2H_2$  and  $H_2$  was reported.<sup>[26]</sup> The influence of hydrogen was also reported for the CCVD synthesis of CNTs. Flahaut *et al.*<sup>[27]</sup> identified the optimal content of  $CH_4$  in mixture with  $H_2$  for the synthesis of DWCNTs. The yield of DWCNTs increased as well as the formation of carbon nanofibers when the content of  $CH_4$  was increased from 3 to 30 mol.%. Xiong *et al.*<sup>[28]</sup> synthesized DWCNTs on Fe-Mo/ $MgO$  catalyst when they diluted  $CH_4$  with  $H_2$ . This effect of  $H_2$  was related to the slowing of the processes of decomposition, diffusion, and precipitation of carbon atoms. Biris *et al.*<sup>[29]</sup> showed similar effect of  $H_2$  on the growth of SWCNTs and they proposed a decrease in the size of metal catalyst in hydrogen environment as the explanation. There is no doubt about a significant role of hydrogen in improving the structural quality of

CNT walls, as described in the many works devoted to this effect.<sup>[30–34]</sup>

In the present work, the  $Mo_{12}O_{28}(\mu_2-OH)_{12}\{Co(H_2O)_3\}_4$  cluster molecule with a  $Co_4Mo_{12}$  core was chosen as a precursor of  $MgO$ -supported catalysts. We compared the catalysts prepared by impregnation or combustion methods for the CCVD growth of CNTs from a mixture of  $CH_4$  and  $H_2$  and studied the effects of the composition and rate of the gas flow on the structure of the carbon product.

## 2. Experimental part

### 2.1. Materials

High purity Magnesium oxide  $MgO$  (analytical reagent quality), cobalt (II) acetate  $Co(OOCCH_3)_2 \cdot 4H_2O$  (analytical reagent quality, anhydrous), ammonium heptamolybdate tetrahydrate  $(NH_4)_6Mo_7O_{24} \cdot 4H_2O$  (>99%), acetic acid  $CH_3COOH$  (puriss.), hydrazine sulfate  $N_2H_6SO_4$  (p.a.), magnesium nitrate  $Mg(NO_3)_2 \cdot 6H_2O$  (analytical reagent quality), citric acid  $C_6H_8O_7$  (analytical reagent quality), and hydrochloric acid (puriss. spec.) were used for the synthesis of catalysts and the purification of CNTs. Methane  $CH_4$  (99,95%) and hydrogen  $H_2$  (99,9999%) were used for the growth of CNTs.

### 2.2. Preparation of catalysts

$Mo_{12}O_{28}(\mu_2-OH)_{12}\{Co(H_2O)_3\}_4$  (briefly  $\{Co_4Mo_{12}\}$ ) was synthesized as described in the original work.<sup>[35]</sup> Shortly,  $Co(OOCCH_3)_2 \cdot 4H_2O$  (11.25 g) and  $(NH_4)_6Mo_7O_{24} \cdot 4H_2O$  (3.36 g) were dissolved in diluted acetic acid (290 mL) and hydrazine sulfate (0.62 g) was added to the solution. Polyoxomolybdate  $\{Co_4Mo_{12}\}$  was precipitated after the heating of the solution at 65 °C for three days.

The methods used for the catalyst preparation and the schematic structure of the catalysts are illustrated in Figure 1. The preparation of catalyst by impregnation comprised the following steps: an aqueous suspension of  $\{Co_4Mo_{12}\}$  and commercial  $MgO$  was stirred at 80 °C until the full evaporation of water. The peach-coloured  $\{Co_4Mo_{12}\}/MgO$  sample was dried in air at 80 °C for 12 h. Decomposition of  $\{Co_4Mo_{12}\}/MgO$  at 700 °C in air for 10 min produced the Co-Mo/ $MgO$  catalyst, which structure was already described in details earlier.<sup>[23]</sup> The catalyst prepared by impregnation method is further denoted as *imp*-catalyst. The combustion process consisted of the following steps:  $\{Co_4Mo_{12}\}$  (0.2 g),  $Mg(NO_3)_2 \cdot 6H_2O$  (17.7 g) and citric acid (7.4 g) were dissolved in deionized water (600 mL) and the resultant solution was placed in a muffle furnace preheated at 550 °C and left until dryness. The catalyst prepared by combustion method is further denoted as *comb*-catalyst. We propose it has a solid solution structure<sup>[36]</sup> for  $MgO$  similar to the catalysts obtained using the same procedure<sup>[37]</sup> where Co may be in substitution of  $MgO$  in the  $MgO$  lattice, but this is not possible for Mo. However, during the process,  $CoMoO_4$  or  $MoO_3$  can be formed, then it can be fixed on surface of  $MgO$  but the exact form and location of Co and Mo are unclear. Analysis by atomic emission spectroscopy revealed a content of Co *ca.* ~1 wt.% and Mo *ca.* ~5 wt.% for both catalysts.

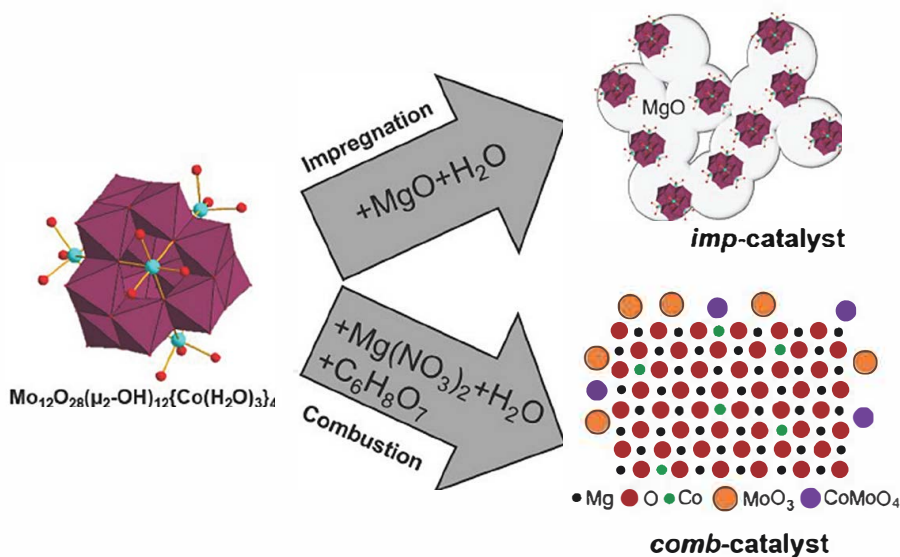


Figure 1. Illustration of impregnation and combustion methods of catalyst formation started from  $\text{Mo}_{12}\text{O}_{28}(\mu_2\text{OH})_{12}\{\text{Co}(\text{H}_2\text{O})_3\}_4$  cluster molecules.

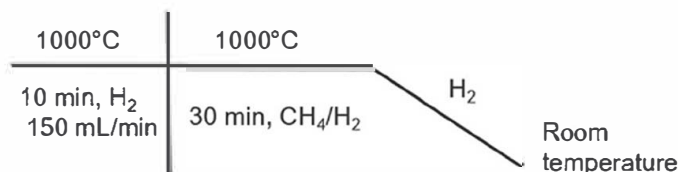


Figure 2. CCVD profile of CNT synthesis.

### 2.3. Synthesis of carbon nanotubes

The procedure for the CNT synthesis was the same for both catalysts and involved three steps shown in Figure 2. A catalyst was distributed in a ceramic boat, which was placed in the cold zone of a quartz tube 4.5 cm in diameter embedded in a horizontal tubular stainless steel reactor of 1 m length. The reactor was filled with hydrogen and heated to 1000 °C. After that, the ceramic boat was introduced into the hot zone of the reactor. The sample was flushed with hydrogen at a flow rate of 150 mL/min to activate the catalyst during 10 min. The CCVD synthesis was carried out in a gaseous mixture of hydrogen and methane with different ratios and flow rates for 30 min. Then, the reactor was flushed with hydrogen (150 mL/min) for 10 min. As a result, black powders were obtained.

The products were treated with a concentrated aqueous solution of HCl to dissolve the MgO support as well as all the accessible metals. Since this acid is a non-oxidizing agent, the used purification treatment does not introduce functional groups on the CNT surface.<sup>[38]</sup> Then CNTs were filtered and washed with distilled water until neutral pH. Finally, CNTs were dried in air at 80 °C for 12 h. In both catalysts, cobalt is the main active metal for CNT growth and CNT yields were calculated as  $\frac{m_{\text{CNTs}}}{m_{\text{Co}}} \times 100\%$ .

### 2.4. Instrumental methods

Transmission electron microscopy (TEM) images were obtained using a JEOL-2010 microscope operated at 200 kV.

Raman spectra were recorded on a LabRAM HR Evolution HORIBA spectrometer using 514 nm  $\text{Ar}^+$  laser radiation.

CNTs were tested as working electrodes in a three-electrode cell to investigate their electrochemical properties. The method of preparation of the electrodes consisted in a homogenization of a CNT sample (5 mg) with a 62 wt. % solution of Teflon F-4D binder in aqueous solution followed by rolling of the mixture in ethanol (a few drops) to form a film. Platinum foil and Ag/AgCl electrode were used as current collector and reference electrode, respectively. The platinum counter electrode and the working electrode were separated with polypropylene membrane impregnated with a 1 M  $\text{H}_2\text{SO}_4$  aqueous solution. Cyclic voltammetry (CV) curves were recorded using a Biologic SP-300 instrument in a potential window from 0 to 1 V at scan rates from 2 to 1000 mV/s. The specific capacity of the electrodes was determined using the formula  $C = A / (V_s \times m)$ , where A is the area under the positive curve,  $V_s$  is the scan rate and m is the mass of carbon material.

## 3. Results and discussion

### 3.1. Impregnation-produced catalyst for CNT synthesis

Typical TEM images of carbon materials synthesized over *imp*-catalyst are shown in Figure 3. Materials contained entangled and bundled CNTs free from amorphous carbon (Figure 3). High-resolution images revealed that the bundles consisted of DWCNTs with an outer diameter ranging from 2 to 5 nm (Figure 3d). These nanotubes were grown when the flow rate of  $\text{CH}_4$  was 200 mL/min. The agglomerates contained individualized MWCNTs and they were formed at all used gaseous flows. The thinnest MWCNTs with an average outer diameter of 5 nm grew at 200 mL/min  $\text{CH}_4$  flow rate (Figure 3d). A decrease in the flow rate to 100 mL/min led to the synthesis of MWCNTs with an outer diameter varying from 5 to 10 nm, with an average value of 8 nm (Figure 3b). MWCNTs with significantly larger diameters up



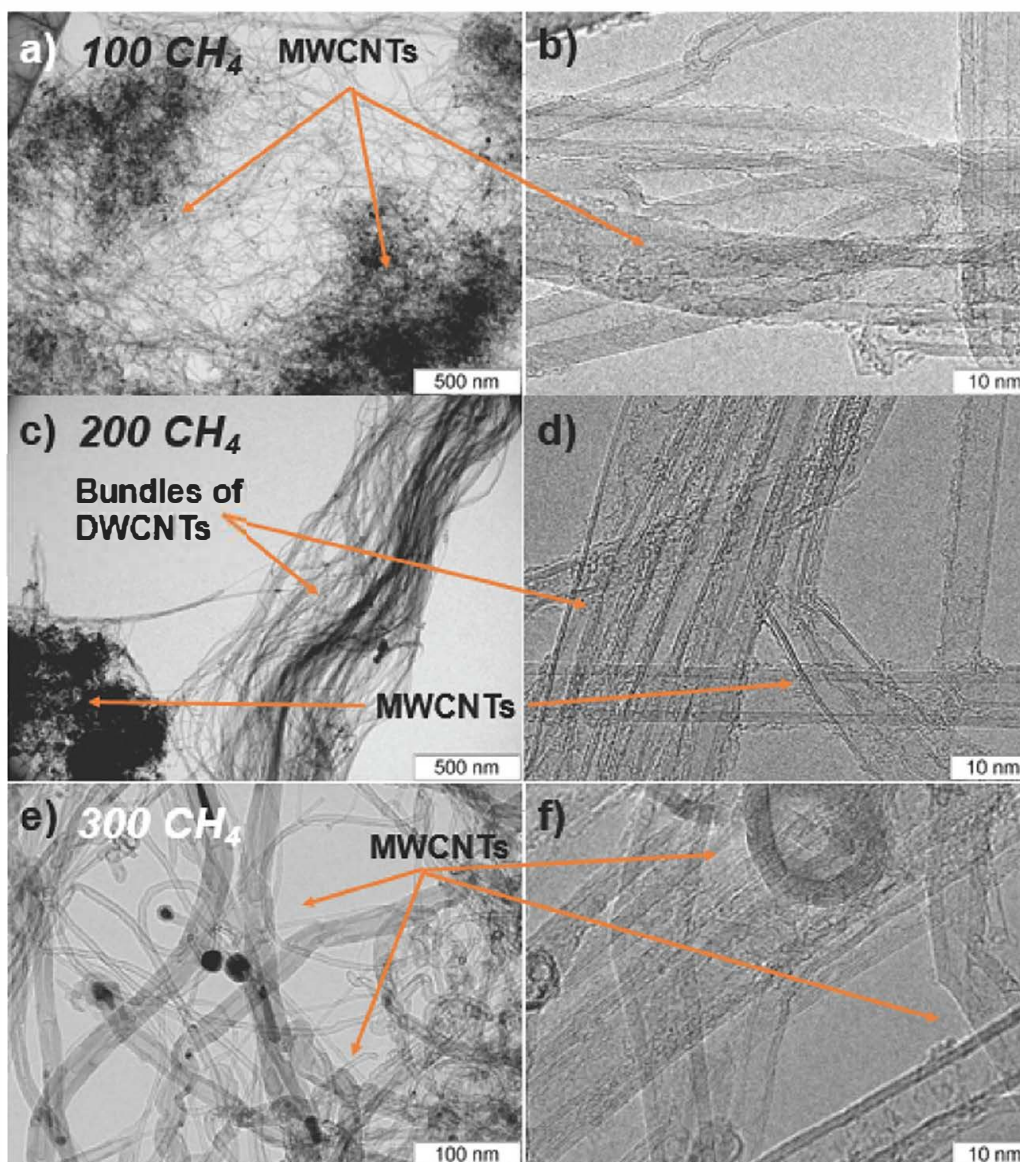


**Figure 3.** Low resolution (a, c, e) and high resolution (b, d, f) TEM images of CNTs synthesized using *imp* catalyst with a flow rate of CH<sub>4</sub> 100 mL/min (a, b), 200 mL/min (c, d) and 300 (e, f).

to 30 nm were formed when the flow rate of CH<sub>4</sub> was increased to 300 mL/min (Figure 3e and f). In this case, metallic nanoparticles were observed within MWCNTs (Figure 3e). High concentration of carbon species in the reaction zone can promote fast growth of CNTs and capture of catalyst with poor adhesion to the support. In previous work the formation of a mixture DWCNTs and MWCNTs was already detected using the same *imp*-catalyst but under a dynamic temperature profile of CCVD process.<sup>[39]</sup>

Raman spectra of the synthesized carbon materials (Figure 4a) revealed the presence of the G-peak at 1580 cm<sup>-1</sup> corresponding to the tangential vibrations of carbon atoms in the graphene plane<sup>[40]</sup> and the disorder-induced D-peak at 1350 cm<sup>-1</sup>.<sup>[41]</sup> The ratio of the integral intensities of D- and G-peaks ( $I_D/I_G$ ) may be used to estimate the disorder in sp<sup>2</sup>-hybridized carbon materials.<sup>[42]</sup> Figure 4b summarizes the data on CNT yield and  $I_D/I_G$  value depending on the CH<sub>4</sub>/H<sub>2</sub> ratio and flow rate. The lowest and highest values of  $I_D/I_G$  ratio were obtained for

the CNTs synthesized with 200 mL/min and 300 mL/min of CH<sub>4</sub>, respectively (Figure 4a). Dilution of methane with hydrogen resulted in a lower yield of CNTs and a decrease or no change in the  $I_D/I_G$  value (Figure 4b). Zhan *et al.* observed a similar trend for the CNT yield when the rate of CH<sub>4</sub> flow increased with a constant H<sub>2</sub> flow.<sup>[43]</sup> An improvement of the atomic ordering in CNT walls was reported when the CH<sub>4</sub> flow increased.<sup>[44]</sup> In our experiments, a stationary state near the catalytic centers was achieved at 200 mL/min of CH<sub>4</sub> flow. A change of the flow rate resulted in strongly non-equilibrium growth conditions and the formation of thicker and defective CNTs (Figure 3).

We can conclude that 200 mL/min of CH<sub>4</sub> represents an optimal synthesis condition providing a high yield of CNTs and good structural quality of their walls. When methane was diluted with hydrogen in a ratio 2:1 and 1:1, production of CNTs decreased due to the decrease in carbon concentration during the synthesis. However, improvement of the crystallinity of CNT walls in the presence of H<sub>2</sub> was

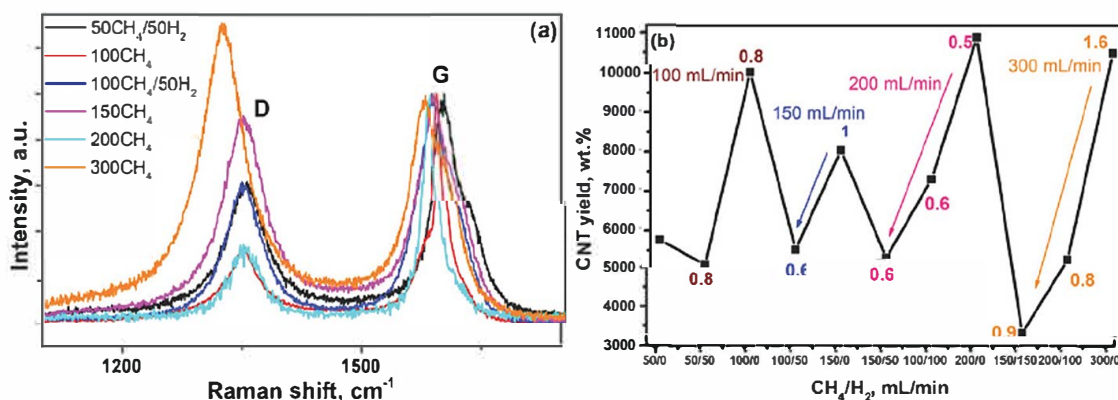


**Figure 4.** (a) Raman spectra of CNTs obtained with *imp* catalyst at 100, 150 and 200 mL/min total CH<sub>4</sub>/H<sub>2</sub> flow rates. (b) Influence of ratio and gas flow rates of CH<sub>4</sub>/H<sub>2</sub> on CNT yield and I<sub>D</sub>/I<sub>G</sub> values (shown by bold numbers). The direction of the arrows indicates a decrease in CNT yield when CH<sub>4</sub> was diluted with H<sub>2</sub> (for a given total flow rate).

evidenced at 150 mL/min and 300 mL/min total flow rates of CH<sub>4</sub>/H<sub>2</sub>. At other flow rates, there was no effect of H<sub>2</sub> addition on the disorder of the CNT structure. Ohashi *et al.* proposed that the addition of H<sub>2</sub> to CH<sub>4</sub> is the necessary condition to synthesize CNTs free from amorphous carbon and an optimum concentration of H<sub>2</sub> in CH<sub>4</sub> was about 1:1.<sup>[45]</sup> Reynolds *et al.*<sup>[46]</sup> obtained the highest CNT yields when 700 sccm of CH<sub>4</sub> were mixed with 200-300 sccm of H<sub>2</sub>. In our experiments, H<sub>2</sub> performed two main roles for CNT formation. One of them was dilution of methane that led to decreasing the CNT yield, and the other was the stabilization effect of CH<sub>4</sub> during the decomposition which promoted a decreasing density of defects in CNTs.

### 3.2. Combustion-produced catalyst for CNT synthesis

TEM study of the product obtained using the *comb*-catalyst and CH<sub>4</sub> with a flow rate of 200 mL/min revealed highly dispersed thin CNTs (Figure 5a). High-resolution TEM images evidenced the co-existence of DWCNTs, triple-walled CNTs (TWCNTs), and MWCNTs (Figure 5b). The average outer diameter of these CNTs was 3 nm, 5 nm and 8 nm, respectively. However, MWCNTs with a larger outer diameter of ~16 nm were also observed in the sample. Note that DWCNTs were not bundled, contrary to what was obtained for the use of *imp*-catalyst in the synthesis (Figure 3c and d). When the rate of CH<sub>4</sub> flow was increased to 300 mL/min, the DWCNTs formed thin bundles (Figure 5c and d). The growth of SWCNTs, DWCNTs and TWCNTs is typical for catalysts prepared by combustion method.<sup>[13]</sup> An optimal composition of the catalyst, which provides prevalence of DWCNTs in the CNT mixture is Mg<sub>0.99</sub>(Co<sub>0.75</sub>Mo<sub>0.25</sub>)<sub>0.01</sub>O<sub>3.6</sub><sup>[36]</sup> and an increase in the content of Mo leads to an increase in the number of CNT walls.<sup>[37]</sup>

The I<sub>D</sub>/I<sub>G</sub> ratios determined from Raman spectra of carbon products varied from 0.2 to 0.8 (Figure 6a). These values are smaller as compared to those found for the CNTs synthesized over *imp*-catalyst (Figure 4b). Figure 6b shows CNT yields depending on the ratio and gas flow rates of CH<sub>4</sub>/H<sub>2</sub>. As in the previous case, the yield decreased when methane was diluted with hydrogen. The highest CNT yield was obtained at 150 mL/min of CH<sub>4</sub> flow rate and the

lowest yield was reached using CH<sub>4</sub>/H<sub>2</sub> with 50/50 mL/min. The I<sub>D</sub>/I<sub>G</sub> ratio was 0.5 for the former product and 0.2 for the latter one. However, the highest I<sub>D</sub>/I<sub>G</sub> ratio was observed at 300 mL/min flow rate of CH<sub>4</sub>. This can be assigned to a decrease in the number of DWCNTs and an increase in the fraction of large-diameter MWCNTs (Figure 5c and d) due to deviation of the synthesis conditions from the stationary state, similarly to what was also observed with the *imp*-catalyst.

Rao *et al.*<sup>[47]</sup> reported that H<sub>2</sub> did not affect the yield of SWCNTs at 800 °C, however, the yield increased when the ratio of H<sub>2</sub>/CH<sub>4</sub> was equal to one at 900 °C. Usually, SWCNT synthesis does not occur without H<sub>2</sub>, which is needed to decrease the decomposition rate of CH<sub>4</sub> and hence to prevent catalyst encapsulation with carbon. Our Raman data show that the ratio and flow-rates of CH<sub>4</sub>/H<sub>2</sub> had an effect on the diameter distribution of SWCNTs and DWCNTs, with radial breathing modes (RBMs) that appeared from 80 to 300 cm<sup>-1</sup>.<sup>[48]</sup> Positions of RBMs are listed in Table S1 and these data indicate the formation of both SWCNTs and DWCNTs independently on the CH<sub>4</sub>/H<sub>2</sub> ratio and flow rate. The use of CH<sub>4</sub> without H<sub>2</sub> provided narrower distributions of CNT diameters which were especially characteristic of low flow rate of CH<sub>4</sub>. We assume that CH<sub>4</sub> has enough reduction ability for the formation of metal particles with a size acceptable for the DWCNT growth. Addition of H<sub>2</sub> to CH<sub>4</sub> increases reduction ability, which leads to the formation of a larger number of catalytically active metal particles, but with a different size distribution. Thus, various SWCNTs and DWCNTs are produced, but the yield of CNTs is decreased due to dilution of CH<sub>4</sub>. However, there are opposite examples in the literature. Orbaek *et al.*<sup>[49]</sup> identified that an increase in the partial pressure of CH<sub>4</sub> higher than 60% in CH<sub>4</sub>/H<sub>2</sub> promoted the carbonization of catalytic particles and decreased the efficiency of the reduction of the catalyst.

### 3.3. Electrochemical properties

The obtained CNTs were tested as electrode materials in electrochemical capacitors. Performances of CNTs synthesized using *comb*-catalysts are illustrated in Figure S2.



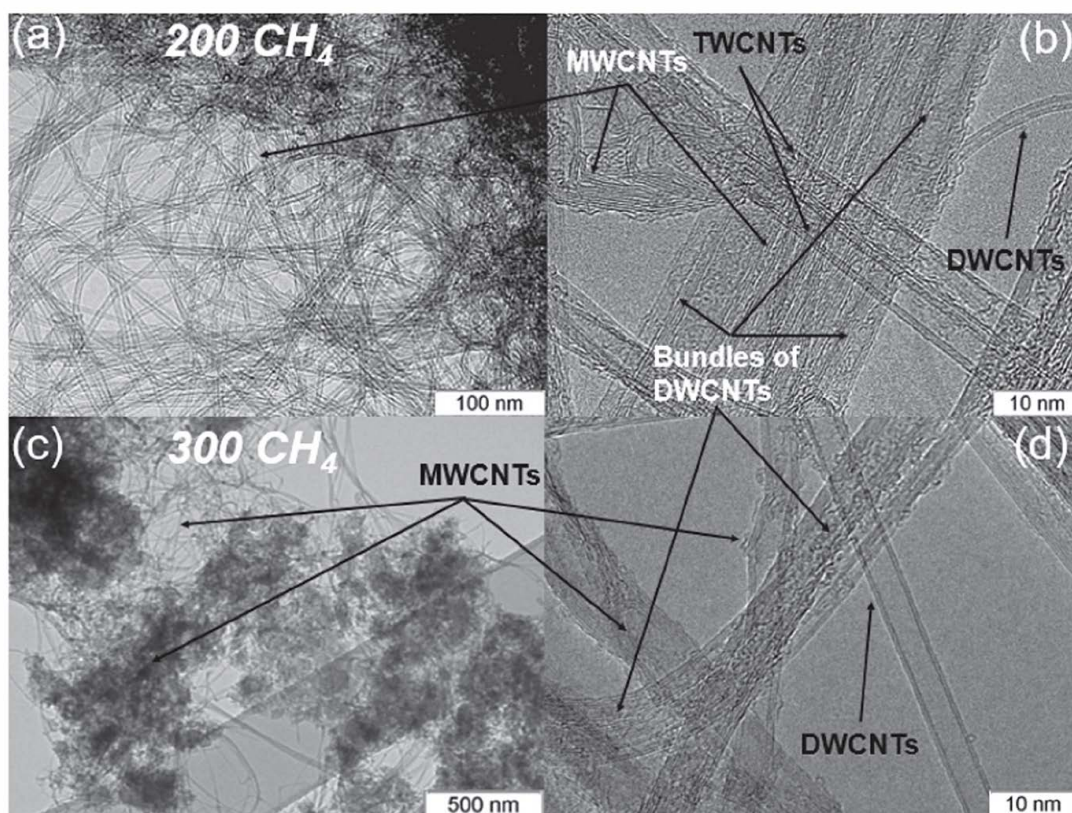


**Figure 5.** Low resolution (a, c) and high resolution (b, d) TEM images of DWCNTs, TWCNTs and MWCNTs synthesized using *comb* catalyst with  $\text{CH}_4$  flow rate of 200 mL/min (a, b) and 300 mL/min (c, d).

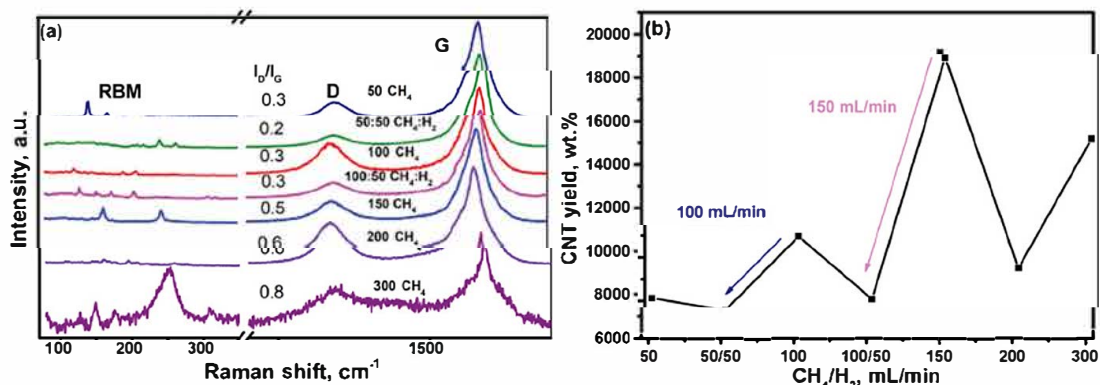


**Figure 6.** (a) Raman spectra of CNTs obtained using *comb* catalyst at different  $\text{CH}_4/\text{H}_2$  ratio and flow rates. (b) CNT yields depending on ratio and gas flow rates of  $\text{CH}_4/\text{H}_2$ . The direction of the arrows indicates decreasing of yields when  $\text{CH}_4$  is diluted with  $\text{H}_2$ .

Typically, the specific capacitance of all electrodes increased with decreasing scan rates due to electrolyte ions having more time to diffuse into the volume of the samples. The CNTs synthesized at 150 mL/min flow-rate of  $\text{CH}_4$  exhibited the best performance at all scan rates, which could be due to a large fraction of MWCNTs in this sample.

Samples obtained in the same synthesis conditions (200 mL/min of  $\text{CH}_4$ ) using different catalysts were selected for a comparative analysis of their electrochemical performances (Figure 7). CNTs synthesized using the *imp*-catalyst exhibited the higher values of specific capacitance at all used scan rates. Specific surface area (SSA) and wettability of the material have the largest impact on the capacitance at high scan rates due to the lack of time for complete diffusion of electrolyte ions. The *imp*-catalyst produced the CNTs

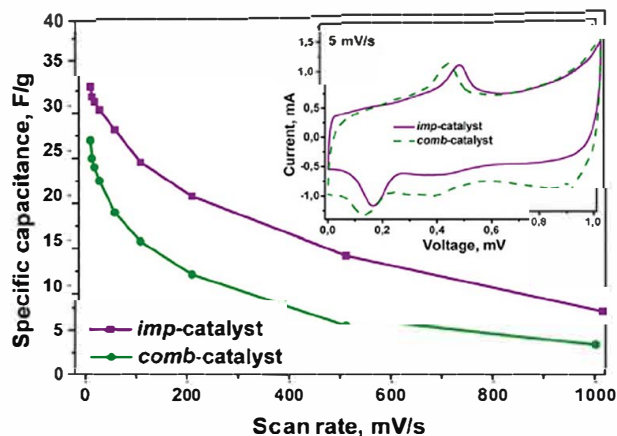


**Figure 7.** Specific capacitance as a function of scan rate of CNTs obtained with *comb* prepared catalyst and *imp* prepared catalysts at 200 mL/min of  $\text{CH}_4$  flow rate.

possessing SSA of  $382\text{ m}^2/\text{g}$ , which is markedly larger than the value of  $290\text{ m}^2/\text{g}$  for CNTs synthesized using the *comb*-catalyst. At low scan rates, redox processes can provide a significant contribution to the electrochemical capacitance. The CV curves of the samples measured at a scan rate of  $5\text{ mV/s}$  (insert in Figure 7) exhibited the peaks at  $\sim 500\text{ mV}$  on the charge curve and  $\sim 200\text{ mV}$  on the discharge curve corresponding to redox processes associated with the reduction of  $\text{Mo}^{6+}$  to intermediate  $\text{MoO}_x$  oxides ( $2.5 < x < 3$ ).<sup>[50]</sup> A shift between the peaks on the charge curves of the samples can be a sign of the difference of Mo states in *imp*-catalyst and *comb*-catalyst. The same redox reactions were observed in our previous work and their occurrence was attributed to the etching of CNT ends during the CV tests.<sup>[39]</sup> It should be noted that areas of redox peaks for both samples are very similar. Thus, it is reasonable to assume that difference in specific capacitance arises from SSA of the samples. The *imp*-catalyst produced DWCNT bundles and MWCNTs with thin walls (Figure 3c and d). Raman spectrum of the sample synthesized using the *comb*-catalyst revealed many low-intensity RBM peaks (Figure 6a) corresponding to SWCNTs and/or DWCNTs. However, TEM images revealed the prevalence of MWCNTs in this sample (Figure 5b). Some of the MWCNTs have thick walls and this may be a reason for the smaller SSA of the sample, causing its lower capacitance.

#### 4. Conclusions

Two types of catalysts were prepared from  $\text{Mo}_{12}\text{O}_{28}(\mu_2\text{-OH})_{12}\{\text{Co}(\text{H}_2\text{O})_3\}_4$  on MgO supports by impregnation or combustion methods. The catalysts were pretreated in reducing atmosphere at  $1000^\circ\text{C}$  during 10 min. CCVD syntheses of CNTs were carried out at different flow-rates of  $\text{CH}_4/\text{H}_2$  during 30 min at  $1000^\circ\text{C}$ . The yield of CNTs strongly depended on the addition of hydrogen and decreased when methane was diluted by hydrogen. TEM images revealed the formation of entangled and bundled CNTs in the case of the *imp*-catalyst, whereas individual CNTs were obtained using the *comb*-catalyst. According to Raman spectroscopy data, SWCNTs and/or DWCNTs were synthesized over the latter catalyst independently on the feeding gas composition and flow rate. Moreover, the  $I_D/I_G$  ratios indicated formation of less disordered CNTs in that case as compared to CNTs grown on the *imp*-catalyst. The thicker and more disordered CNTs grew on both catalysts with an increase in  $\text{CH}_4$  flow rate. An addition of hydrogen to methane enlarged the diameter distribution of SWCNTs or DWCNTs due to the formation of catalytically active metal particles of different sizes. The electrochemical performances of CNTs obtained using two different catalysts at the same synthesis parameters were compared in  $1\text{ M H}_2\text{SO}_4$  electrolyte. The CNTs synthesized using the *imp*-catalyst exhibited a higher specific capacitance at all used scan rates mainly due to the presence of thin-wall MWCNTs, providing a large surface area for electrolyte ion adsorption.

#### Acknowledgments

We are grateful to Mr. B.A. Kolesov for the Raman analysis and Mr. P. Lonchambon for the help in the combustion synthesis of catalysts.

#### Disclosure statement

No potential conflict of interest was reported by the author(s).

#### Funding

The work was supported by the Russian Foundation for Basic Research (grant № 18 33 01053). Mrs V.R. Kuznetsova thanks grant № 004 HCF 19 from Novosibirsk State Technical University.

#### References

- [1] Dupuis, A. C. The Catalyst in the CCVD of Carbon Nanotubes a Review. *Prog. Mater. Sci.* **2005**, *50*, 929–961. DOI: 10.1016/j.pmatsci.2005.04.003.
- [2] Tessonier, J. P.; Su, D. S. Recent Progress on the Growth Mechanism of Carbon Nanotubes: A Review. *ChemSusChem* **2011**, *4*, 824–847. DOI: 10.1002/cssc.201100175.
- [3] Azam, M. A.; Zulkapli, N. N.; Nawi, Z. M.; Azren, N. M. Systematic Review of Catalyst Nanoparticles Synthesized by Solution Process: Towards Efficient Carbon Nanotube Growth. *J. Sol Gel Sci. Technol.* **2015**, *73*, 484–500. DOI: 10.1007/s10971-014-3600-5.
- [4] Yang, Y.; Zhang, H.; Yan, Y. Synthesis of Carbon Nanotube on Stainless Steel Microfibrous Composite Comparison of Direct and Indirect Growth and Its Application in Fixed Bed m Cresol Adsorption. *Chem. Eng. Res. Des.* **2018**, *139*, 162–173. DOI: 10.1016/j.cherd.2018.09.027.
- [5] Parsian, S.; Shahidi, S.; Mirjalili, M.; Ghoranneviss, M. In Situ Synthesis of Carbon Nanotubes on Glass Mat Using Thermal Chemical Vapor Deposition Method. *Fullerenes, Nanotub. Carbon Nanostruct.* **2018**, *26*, 551–556. DOI: 10.1080/1536383X.2018.1457650.
- [6] Shah, K. A.; Tali, B. A. Synthesis of Carbon Nanotubes by Catalytic Chemical Vapour Deposition: A Review on Carbon Sources, Catalysts and Substrates. *Mater. Sci. Semicond. Process* **2016**, *41*, 67–82. DOI: 10.1016/j.mssp.2015.08.013.
- [7] Chai, S. P.; Zein, S. H. S.; Mohamed, A. R. Preparation of Carbon Nanotubes over Cobalt Containing Catalysts via Catalytic Decomposition of Methane. *Chem. Phys. Lett.* **2006**, *426*, 345–350. DOI: 10.1016/j.cplett.2006.05.026.
- [8] Qingwen, L.; Hao, Y.; Yan, C.; Jin, Z.; Zhongfan, L. A Scalable CVD Synthesis of High Purity Single Walled Carbon Nanotubes with Porous MgO as Support Material. *J. Mater. Chem.* **2002**, *12*, 1179–1183. DOI: 10.1039/b109763f.
- [9] Triantafyllidis, K. S.; Karakoulia, S. A.; Gournis, D.; Delimitis, A.; Nalbandian, L.; Maccallini, E.; Rudolf, P. Formation of Carbon Nanotubes on Iron/Cobalt Oxides Supported on Zeolite Y: Effect of Zeolite Textural Properties and Particle Morphology. *Microporous Mesoporous Mater.* **2008**, *110*, 128–140. DOI: 10.1016/j.micromeso.2007.10.007.
- [10] Gulino, G.; Vieira, R.; Amadou, J.; Nguyen, P.; Ledoux, M. J.; Galvagno, S.; Centi, G.; Pham Huu, C.  $\text{C}_2\text{H}_6$  as an Active Carbon Source for a Large Scale Synthesis of Carbon Nanotubes by Chemical Vapour Deposition. *Appl. Catal. A Gen.* **2005**, *279*, 89–97. DOI: 10.1016/j.apcata.2004.10.016.
- [11] Harutyunyan, A. R.; Pradhan, B. K.; Kim, U. J.; Chen, G.; Eklund, P. C. CVD Synthesis of Single Wall Carbon Nanotubes under “Soft” Conditions. *Nano Lett.* **2002**, *2*, 525–530. DOI: 10.1021/nl0255101.



- [12] Kitiyanan, B.; Alvarez, W.; Harwell, J. H.; Resasco, D. E. Controlled Production of Single Wall Carbon Nanotubes by Catalytic Decomposition of CO on Bimetallic Co Mo Catalysts. *Chem. Phys. Lett.* **2000**, *317*, 497–503. DOI: 10.1016/S0009-2614(99)01379-2.
- [13] Flahaut, E.; Laurent, C.; Peigney, A. Catalytic CVD Synthesis of Double and Triple Walled Carbon Nanotubes by the Control of the Catalyst Preparation. *Carbon* **2005**, *43*, 375–383. DOI: 10.1016/j.carbon.2004.09.021.
- [14] Müller, A.; Krickemeyer, E.; Bögge, H.; Schmidtman, M.; Peters, F. Organizational Forms of Matter: An Inorganic Super Fullerene and Keplerate Based on Molybdenum Oxide. *Angew. Chemie Int. Ed.* **1998**, *37*, 3359–3363. DOI: 10.1002/(SICI)1521-3773(19981231)37:24 < 3359::AID-ANIE3359 > 3.0.CO; 2 J.
- [15] An, L.; Owens, J. M.; McNeil, L. E.; Liu, J. Synthesis of Nearly Uniform Single Walled Carbon Nanotubes Using Identical Metal Containing Molecular Nanoclusters as Catalysts. *J. Am. Chem. Soc.* **2002**, *124*, 13688–13689. DOI: 10.1021/ja0274958.
- [16] Müller, A.; Sarkar, S.; Shah, S. Q. N.; Bögge, H.; Schmidtman, M.; Sarkar, S.; Kögerler, P.; Hauptfleisch, B.; Trautwein, A. X.; Schünemann, V. Archimedean Synthesis and Magic Numbers: "Sizing" Giant Molybdenum Oxide Based Molecular Spheres of the Keplerate Type. *Angew. Chem. Int. Ed.* **1999**, *38*, 3238–3241. DOI: 10.1002/(SICI)1521-3773(19991102)38:21 < 3238::AID-ANIE3238 > 3.0.CO; 2 6.
- [17] Yang, F.; Wang, X.; Si, J.; Zhao, X.; Qi, K.; Jin, C.; Zhang, Z.; Li, M.; Zhang, D.; Yang, J.; et al. Water Assisted Preparation of High Purity Semiconducting (14,4) Carbon Nanotubes. *ACS Nano* **2017**, *11*, 186–193. DOI: 10.1021/acsnano.6b06890.
- [18] Huang, S.; Fu, Q.; An, L.; Liu, J. Growth of Aligned SWNT Arrays from Water Soluble Molecular Clusters for Nanotube Device Fabrication. *Phys. Chem. Chem. Phys.* **2004**, *6*, 1077. DOI: 10.1039/b315892f.
- [19] Anderson, R. E.; Colorado, R.; Crouse, C.; Ogrin, D.; Maruyama, B.; Pender, M. J.; Edwards, C. L.; Whitsitt, E.; Moore, V. C.; Koveal, D.; et al. A Study of the Formation, Purification and Application as a SWNT Growth Catalyst of the Nanocluster  $[H_xPMo_{12}O_{40}C_4H_4Mo_{72}Fe_{30}(O_2CMe)_{15}O_{254}(H_2O)_{98}]$ . *Dalton Trans.* **2006**, (25), 3097–3107. DOI: 10.1039/B518395B.
- [20] Edgar, K.; Spencer, J. L. The Synthesis of Carbon Nanotubes from Müller Clusters. *Curr. Appl. Phys.* **2006**, *6*, 419–421. DOI: 10.1016/j.cap.2005.11.032.
- [21] Goss, K.; Kamra, A.; Spudat, C.; Meyer, C.; Kögerler, P.; Schneider, C. M. CVD Growth of Carbon Nanotubes Using Molecular Nanoclusters as Catalyst. *Phys. Status Solidi B.* **2009**, *246*, 2494–2497. DOI: 10.1002/pssb.200982320.
- [22] Lobiak, E. V.; Shlyakhova, E. V.; Guse'nikov, A. V.; Plyusnin, P. E.; Shubin, Y. V.; Okotrub, A. V.; Bulusheva, L. G. Carbon Nanotube Synthesis Using Fe Mo/MgO Catalyst with Different Ratios of CH<sub>4</sub> and H<sub>2</sub> Gases. *Phys. Status Solidi B* **2018**, *255*, 1700274. DOI: 10.1002/pssb.201700274.
- [23] Lobiak, E. V.; Shlyakhova, E. V.; Bulusheva, L. G.; Plyusnin, P. E.; Shubin, Y. V.; Okotrub, A. V. Ni Mo and Co Mo Alloy Nanoparticles for Catalytic Chemical Vapor Deposition Synthesis of Carbon Nanotubes. *J. Alloys Compd.* **2015**, *621*, 351–356. DOI: 10.1016/j.jallcom.2014.09.220.
- [24] Jourdain, V.; Bichara, C. Current Understanding of the Growth of Carbon Nanotubes in Catalytic Chemical Vapour Deposition. *Carbon* **2013**, *58*, 2–39. DOI: 10.1016/j.carbon.2013.02.046.
- [25] Wang, X. K.; Lin, X. W.; Mesleh, M.; Jarrold, M. F.; Dravid, V. P.; Ketterson, J. B.; Chang, R. P. H. The Effect of Hydrogen on the Formation of Carbon Nanotubes and Fullerenes. *J. Mater. Res.* **1995**, *10*, 1977–1983. DOI: 10.1557/JMR.1995.1977.
- [26] Zhao, X.; Ohkohchi, M.; Wang, M.; Iijima, S.; Ichihashi, T.; Ando, Y. Preparation of High Grade Carbon Nanotubes by Hydrogen Arc Discharge. *Carbon* **1997**, *35*, 775–781. DOI: 10.1016/S0008-6223(97)00033-X.
- [27] Flahaut, E.; Peigney, A.; Laurent, C. Double Walled Carbon Nanotubes in Composite Powders. *J. Nanosci. Nanotechnol.* **2003**, *3*, 151–158. DOI: 10.1166/jnn.2003.177.
- [28] Xiong, G. Y.; Suda, Y.; Wang, D. Z.; Huang, J. Y.; Ren, Z. F. Effect of Temperature, Pressure, and Gas Ratio of Methane to Hydrogen on the Synthesis of Double Walled Carbon Nanotubes by Chemical Vapour Deposition. *Nanotechnology* **2005**, *16*, 532–535. DOI: 10.1088/0957-4484/16/4/033.
- [29] Biris, A. R.; Li, Z.; Dervishi, E.; Lupu, D.; Xu, Y.; Saini, V.; Watanabe, F.; Biris, A. S. Effect of Hydrogen on the Growth and Morphology of Single Wall Carbon Nanotubes Synthesized on a FeMo/MgO Catalytic System. *Phys. Lett. A.* **2008**, *372*, 3051–3057. DOI: 10.1016/j.physleta.2008.01.023.
- [30] Sharma, A. K.; Sharma, R.; Chaudhary, U. Hydrogen Acetylene Gas Ratio and Catalyst Thickness Effect on the Growth of Uniform Layer of Carbon Nanotubes. *Fullerenes, Nanotub. Carbon Nanostruct.* **2017**, *25*, 397–403. DOI: 10.1080/1536383X.2017.1320545.
- [31] Castro, C.; Pinault, M.; Porterat, D.; Reynaud, C.; Mayne L'Hermite, M. The Role of Hydrogen in the Aerosol Assisted Chemical Vapor Deposition Process in Producing Thin and Densely Packed Vertically Aligned Carbon Nanotubes. *Carbon* **2013**, *61*, 585–594. DOI: 10.1016/j.carbon.2013.05.040.
- [32] Behr, M. J.; Gauding, E. A.; Mkhoyan, K. A.; Aydil, E. S. Effect of Hydrogen on Catalyst Nanoparticles in Carbon Nanotube Growth. *J. Appl. Phys.* **2010**, *108*, 53303. DOI: 10.1063/1.3467971.
- [33] Chinthaginjala, J. K.; Lefferts, L. Influence of Hydrogen on the Formation of a Thin Layer of Carbon Nanofibers on Ni Foam. *Carbon* **2009**, *47*, 3175–3183. DOI: 10.1016/j.carbon.2009.07.025.
- [34] Zhang, H.; Cao, G.; Wang, Z.; Yang, Y.; Shi, Z.; Gu, Z. Influence of Ethylene and Hydrogen Flow Rates on the Wall Number, Crystallinity, and Length of Millimeter Long Carbon Nanotube Array. *J. Phys. Chem. C.* **2008**, *112*, 12706–12709. DOI: 10.1021/jp802998v.
- [35] Müller, A.; Beugholt, C.; Kögerler, P.; Bögge, H.; Bud'ko, S.; Luban, M.  $[Mo^V_{12}O_{30}(\mu_2 OH)_{10}H_2[Ni^{II}(H_2O)_3]_4]$ , a Highly Symmetrical  $\epsilon$  Keggin Unit Capped with Four Ni<sup>II</sup> Centers: Synthesis and Magnetism. *Inorg. Chem.* **2000**, *39*, 5176–5177. DOI: 10.1021/ic0005285.
- [36] Flahaut, E.; Bacsca, R.; Peigney, A.; Laurent, C. Gram Scale CCVD Synthesis of Double Walled Carbon Nanotubes. *Chem. Commun.* **2003**, (12), 1442. DOI: 10.1039/b301514a.
- [37] Flahaut, E.; Peigney, A.; Bacsca, W. S.; Bacsca, R. R.; Laurent, C. CCVD Synthesis of Carbon Nanotubes from (Mg,Co,Mo)O Catalysts: Influence of the Proportions of Cobalt and Molybdenum. *J. Mater. Chem.* **2004**, *14*, 646. DOI: 10.1039/b312367g.
- [38] Lavskaya, Y. V.; Bulusheva, L. G.; Okotrub, A. V.; Yudanov, N. F.; Vyalikh, D. V.; Fonseca, A. Comparative Study of Fluorinated Single and Few Wall Carbon Nanotubes by X Ray Photoelectron and X Ray Absorption Spectroscopy. *Carbon* **2009**, *47*, 1629–1636. DOI: 10.1016/j.carbon.2009.01.046.
- [39] Lobiak, E. V.; Bulusheva, L. G.; Galitsky, A. A.; Smirnov, D. A.; Flahaut, E.; Okotrub, A. V. Structure and Electrochemical Properties of Carbon Nanotubes Synthesized with Catalysts Obtained by Decomposition of Co, Ni, and Fe Polyoxomolybdates Supported by MgO. *J. Struct. Chem.* **2018**, *59*, 786–792. DOI: 10.1134/S0022476618040066.
- [40] Choi, Y. C.; Min, K. I.; Jeong, M. S. Novel Method of Evaluating the Purity of Multiwall Carbon Nanotubes Using Raman Spectroscopy. *J. Nanomater.* **2013**, *2013*, 1–6. DOI: 10.1155/2013/615915.
- [41] Dresselhaus, M. S.; Jorio, A.; Souza Filho, A. G.; Saito, R. Defect Characterization in Graphene and Carbon Nanotubes Using Raman Spectroscopy. *Proc. R. Soc. A.* **2010**, *368*, 5355–5377. DOI: 10.1098/rsta.2010.0213.
- [42] Antunes, E. F.; Lobo, A. O.; Corat, E. J.; Trava Airoldi, V. J. Influence of Diameter in the Raman Spectra of Aligned Multi

- Walled Carbon Nanotubes. *Carbon* **2007**, *45*, 913–921. DOI: 10.1016/j.carbon.2007.01.003.
- [43] Zhan, S.; Tian, Y.; Cui, Y.; Wu, H.; Wang, Y.; Ye, S.; Chen, Y. Effect of Process Conditions on the Synthesis of Carbon Nanotubes by Catalytic Decomposition of Methane. *China Particul.* **2007**, *5*, 213–219. DOI: 10.1016/j.cpart.2007.03.004.
- [44] Chai, S. P.; Seah, C. M.; Mohamed, A. R. A Parametric Study of Methane Decomposition into Carbon Nanotubes over 8Co/2Mo/Al<sub>2</sub>O<sub>3</sub> Catalyst. *J. Nat. Gas Chem.* **2011**, *20*, 84–89. DOI: 10.1016/S1003-9953(10)60151-X.
- [45] Ohashi, F.; Chen, G. Y.; Stolojan, V.; Silva, S. R. P. The Role of the Gas Species on the Formation of Carbon Nanotubes during Thermal Chemical Vapour Deposition. *Nanotechnol.* **2008**, *19*, 445605. DOI: 10.1088/0957-4484/19/44/445605.
- [46] Reynolds, C.; Duong, B.; Seraphin, S. Effects of Hydrogen Flow Rate on Carbon Nanotube Growth. *J. Undergrad. Res. Phys.* **2010**, *23*, 1–11.
- [47] Rao, F. B.; Li, T.; Wang, Y. L. Effect of Hydrogen on the Growth of Single Walled Carbon Nanotubes by Thermal Chemical Vapor Deposition. *Phys. E Low Dimensional Syst. Nanostruct.* **2008**, *40*, 779–784. DOI: 10.1016/j.physe.2007.09.185.
- [48] Dresselhaus, M. S.; Dresselhaus, G.; Saito, R.; Jorio, A. Raman Spectroscopy of Carbon Nanotubes. *Phys. Rep.* **2005**, *409*, 47–99. DOI: 10.1016/j.physrep.2004.10.006.
- [49] Orbaek, A. W.; Owens, A. C.; Barron, A. R. Increasing the Efficiency of Single Walled Carbon Nanotube Amplification by Fe/Co Catalysts through the Optimization of CH<sub>4</sub>/H<sub>2</sub> Partial Pressures. *Nano Lett.* **2011**, *11*, 2871–2874. DOI: 10.1021/nl201315j.
- [50] Martínez Huerta, M. V.; Rodríguez, J. L.; Tsiouvaras, N.; Peña, M. A.; Fierro, J. L. G.; Pastor, E. Novel Synthesis Method of CO Tolerant PtRu/MoO<sub>x</sub> Nanoparticles: Structural Characteristics and Performance for Methanol Electrooxidation. *Chem. Mater.* **2008**, *20*, 4249–4259. DOI: 10.1021/cm703047p.

Supplemental file

**Effect of Co-Mo catalyst preparation and CH<sub>4</sub>/H<sub>2</sub> flow on carbon nanotube synthesis**

Lobiak E.V.<sup>1</sup>, Kuznetsova V.R.<sup>1,2</sup>, Flahaut E.<sup>3</sup>, Okotrub A.V.<sup>1</sup>,  
Bulusheva L.G.<sup>1</sup>

<sup>1</sup>*Nikolaev Institute of Inorganic Chemistry SB RAS, Novosibirsk, Russia*

<sup>2</sup>*Novosibirsk State Technical University, Novosibirsk, Russia*

<sup>3</sup>*CNRS, Institut Carnot Cirimat, F-31062 Toulouse, France*

Lobiak E.V. [lobiakev@niic.sbras.ru](mailto:lobiakev@niic.sbras.ru) Nikolaev Institute of Inorganic Chemistry SB RAS,  
Novosibirsk, Russia



Ratio of CH <sub>4</sub> /H <sub>2</sub> mixture, mL/min	RBM position, cm <sup>-1</sup>
50/0	138, 209.3, 218.5, 164.5, 162
50/50	87-92-97,2-103,4-105,5 109-127,6-134,5-138,7-141,4-147,6-157,3-164,9-168,4-176,6-179,3 201,4-209-218-240,8-262,9
100/0	119,8-189,2-207
100/50	127,7-151,6-155,4-166,6-173,3-183-204,8 239,2-249,7-256,4 307,9-319,9
150/0	146.2-152.5-161.4 243.5-260.8
200/0	160.4-167.7-174-176.4-194.8-202.2-209.7-218.2-221.2-223 259-262-265-267.2-272.4
300/0	127.6-149-175.9 252, 308, 314

**Table S1.**

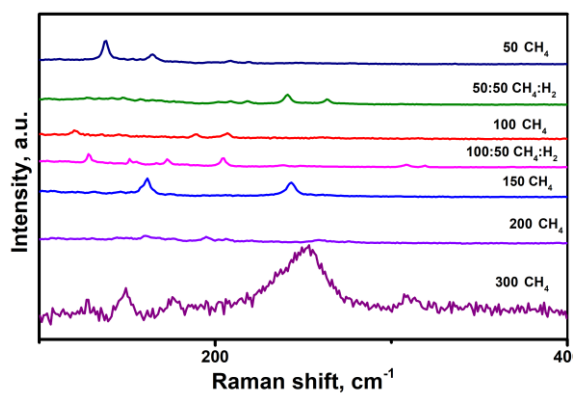


**Figure S1.**

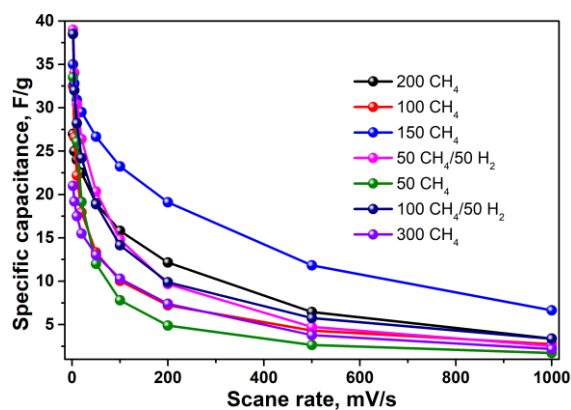


**Figure S2.**

**Table S1.** RBM positions of CNTs synthesized using *comb*-prepared catalyst at different CH<sub>4</sub>/H<sub>2</sub> ratios and flow rates.

**Fig. S1.** RBM Raman spectra peaks of CNTs synthesized using *comb*-prepared catalyst at different CH<sub>4</sub>/H<sub>2</sub> ratios and flow rates.

**Fig. S2.** Specific capacitance as a function of scan rate of CNTs obtained with *comb*-prepared catalyst at different CH<sub>4</sub>/H<sub>2</sub> ratios and flow rates.